

1 **Optimizing the electrical excitation of an atmospheric pressure plasma advanced
2 oxidation process.**

3

4 P. Olszewski¹, J.F. Li², D. X. Liu², J. L. Walsh^{1*}

5

6 ¹ *Department of Electrical Engineering and Electronics, University of Liverpool, L69 3BX, UK*

7

8 ² *State Key Laboratory of Electrical Insulation and Power Equipment, Xi'an Jiaotong University,
9 710049, P. R. China*

10

11

12 **Abstract**

13

14 The impact of pulse-modulated generation of atmospheric pressure plasma on the efficiency
15 of organic dye degradation has been investigated. Aqueous samples of methyl orange were
16 exposed to low temperature air plasma and the degradation efficiency was determined by
17 absorbance spectroscopy. The plasma was driven at a constant frequency of 35 kHz with a
18 duty cycle of 25 %, 50 %, 75 % and 100 %. Relative concentrations of dissolved nitrogen
19 oxides, pH, conductivity and the time evolution of gas phase ozone were measured to identify
20 key parameters responsible for the changes observed in degradation efficiency. The results
21 indicate that pulse modulation significantly improved dye degradation efficiency, with a plasma
22 pulsed at 25 % duty showing a two-fold enhancement. Additionally, pulse modulation led to a
23 reduction in the amount of nitrate contamination added to the solution by the plasma. The
24 results clearly demonstrate that optimization of the electrical excitation of the plasma can
25 enhance both degradation efficiency and the final water quality.

26

27 **Keywords:** plasma discharge; water treatment; advanced oxidation.

*Corresponding author: JLWalsh@Liverpool.ac.uk

1 **1. Introduction**

2 Advanced oxidation processes (AOPs) have received considerable interest for wastewater
3 treatment [1]. Of the many AOPs currently under investigation, atmospheric pressure plasma
4 shows great promise as it combines chemical, mechanical and electrical processes with a
5 proven capability for degrading the most intransigent substances; examples include plasma-
6 induced degradation of phenol [2, 3], methylene blue [4, 5], and trace contaminants in tertiary-
7 treated water [6]. Plasma generates an abundance of oxidizing species including OH*, O*,
8 H₂O₂ and O₃ and potentially shockwaves, high temperatures, and large fluxes of UV photons
9 - all of which contribute to the degradation of persistent chemicals [7].

10 Decolorization of organic dyes is a promising area for which plasma-based AOPs have been
11 considered. It is estimated that 12 % of the total 7×10^5 tons of organic dye used annually is
12 discharged into the environment worldwide [8], due mostly to inefficiencies in the dyeing
13 process. Many dyes cannot be degraded using conventional means due to their stable
14 molecular structure [4]. Dyes discharged into the environment disrupt the ecosystem and are
15 toxic to both fauna and flora [8, 9].

16 In plasma-mediated dye decolorization studies, the primary benchmark when comparing
17 reactor designs for industrial feasibility is electrical efficiency [9]. Recently, Malik conducted a
18 review of 27 common types of plasma reactor used to decolorize various dyes [10]. In the
19 study, efficiency was defined as the amount of energy required to reduce the initial dye
20 concentration by 50 %; efficiency yields for the 27 plasma reactors differed by up to five orders
21 of magnitude, highlighting that reactor design and electrical excitation have an enormous
22 impact on the efficiency of the process. Critically, the review by Malik examined data gathered
23 from a wide variety of studies that employed a variety of reactor configurations, plasma
24 generation techniques and dye composition / concentrations. Due to these variations it is
25 difficult to pinpoint the most efficient reactor configuration and excitation technique; however,
26 it is clear that both factors play a major role in determining the efficiency of the system.

27 In terms of optimizing the plasma generating waveform to maximize degradation efficiency
28 Grabowski *et. al.* demonstrated that the efficiency of ozone production in a pin over liquid film
29 reactor can be doubled by changing pulse frequency [2, 3]. Sano *et. al.* found that the
30 discharge polarity in a similar pin over water reactor had a significant effect on phenol
31 degradation [11]. Studies by Simek *et. al.* have shown that ozone production efficiency can be
32 increased by decreasing duty cycle for plasmas generated in pure oxygen and synthetic air
33 [12, 13]. Indeed, many other works in the field of plasma science have demonstrated the ability
34 to tailor the excitation dynamics of a plasma discharge [14]. Essentially, the recent literature

1 on plasma based AOP's indicates that two key factors dictate the efficiency of the process: (1)
2 the design of the reactor, which should be optimized to promote the mass transfer of reactive
3 species and (2) the electrical parameters of the plasma source, which should be optimized to
4 generate an abundance of oxidizing species with minimal energy input.

5 In this contribution, the degradation of methyl orange (MO) in the aqueous phase was
6 optimized using a pulse-modulated surface barrier discharge (SBD) reactor. Pulse modulation
7 of plasma is known to enhance electrical efficiency and minimize undesirable aspects
8 associated with plasma generation; including gas heating and electrode wear [7]. To
9 demonstrate the advantage of pulse modulation, this study systematically investigates pulse
10 waveform parameters including pulse period, pulse repetition rate and input power in order to
11 establish the optimum operating parameters. An SBD reactor generates a layer of plasma on
12 a dielectric surface that is positioned millimeters above the sample surface; as such, it operates
13 on a fundamentally different principle to many of the plasma reactor designs reported in the
14 literature. The SBD configuration does not require the sample solution to act as an electrode
15 hence it is immune to changes in the electrical properties of the sample. Changes in the
16 electrical properties are inevitable during plasma exposure; in direct-contact reactors, these
17 changes influence the plasma dynamics and the degradation efficiency varies accordingly. In
18 the context of this study, it is essential to separate the effects observed through intentional
19 changes to the electrical excitation to those occurring through the drift of the electrical
20 properties of the sample.

21 A drawback of the SBD configuration is the inefficient transport of reactive species from the
22 plasma to the liquid phase; a process which is less efficient than in direct-contact reactors.
23 Since species with high oxidation potentials also have the shortest lifetimes, the spacing
24 between the SBD and sample limits the flux reaching the sample surface and efficiency drops.
25 However, in the context of industrially-viable water treatment, the SBD reactor has significant
26 benefits. Placing electrodes in contact with the sample can lead to further contamination and
27 accelerated electrode wear, a factor deemed to be one of the major obstacles preventing
28 widespread use of plasma AOP's. Direct contact plasma systems commonly involve high
29 pulsed currents, conditions which impact electrode longevity. The remote SBD reactor
30 employed in this study exhibits minimal heating and provides little opportunity for further
31 contamination of the sample solution. The choice of a surface discharge reactor was therefore
32 made for two practical purposes: to allow the consistent study of the effects of the plasma
33 generating waveform on efficiency and because surface discharge reactors are versatile,
34 scalable and practical on an industrial scale.

1 **2. Experimental Setup**

2 *2.1 Apparatus*

3 The plasma reactor used in this study is depicted in figure 1. The SBD electrode employed
4 copper strips adhered to both sides of a 75 mm diameter, 1 mm thick quartz disc, thus forming
5 a dielectric barrier discharge (DBD) configuration. The electrodes placed on one side of the
6 disc were attached to the power source and the electrodes on the opposite side (sample facing)
7 were grounded. The exposed sample in the reactor had a surface area of 56.7 cm² with a
8 separation of 9.4 mm between the grounded electrode and sample surface. The space above
9 the sample liquid had a total volume of 53 mL.

10 The plasma generating source produced a sinusoidal signal at a fixed frequency of 35 kHz and
11 enabled the independent variation of the period and duty cycle of the pulse-modulation
12 envelope. Mean plasma power consumption was determined using the mean of the product
13 between the applied voltage and current over 200 cycles of the applied voltage. Figure 2(a)
14 shows current and voltage waveforms with the SBD operating at a mean power of 5 W. Typical
15 of a DBD operating in a molecular gas, the current waveform exhibits multiple short current
16 peaks, indicating the presence of micro-discharges [15]. High-speed imaging of the discharge
17 formation, also shown in figure 2(a), indicated that the plasma consisted of multiple micro-
18 discharges forming at imperfections on the electrode surface. The area of plasma generation
19 was calculated based on photographs of the system operating at 5 W and was found to be
20 approximately $5.8 \pm 0.5 \text{ cm}^2$.

21

22 *2.2 Reagents*

23 In all experiments, deionised (DI) water from a Purite DC7 deioniser was used. Microscopy
24 grade Fluka methyl orange ($\text{C}_{14}\text{H}_{14}\text{N}_3\text{NaO}_3\text{S}$, Sigma Aldrich 68250-25G) was dissolved in DI
25 water without further modification.

26

27 *2.3 Analysis methods*

28 Decolorization of the dye sample was measured by absorbance spectroscopy using an Ocean
29 Optics USB4000-UV-VIS spectrometer and quartz cuvette. An Ocean Optics DH-2000 UV-
30 VIS-NIR light source was employed to measure absorbance from 200 to 800 nm. Absorbance
31 measurements were conducted in triplicate using 12 mL samples. MO at a concentration of 20
32 mg/L was tested for decolorization at various power and duty cycle settings. Samples were
33 placed in a vial immediately after plasma treatment and sealed. 2 mL aliquots were sampled
34 into a quartz cuvette for absorbance testing and the remainder of the sample was stored in a

1 cool, dark place. Absorbance measurements were taken 5 minutes after the end of each test,
2 with a second measurement being made 24 hours after treatment.

3 All plasma treatments were conducted with a total energy of 1.8 kJ (constant energy density
4 of 150 kJ/L). This was accomplished by adjusting the duration of treatment for the various
5 power cases. For example, tests conducted with a plasma power of 2.5 W were 12 minutes in
6 duration, 5 W tests were 6 minutes in duration and 10 W tests were 3 minutes in duration. The
7 plasma power in continuous tests was adjusted by varying the amplitude of the high voltage
8 sinusoid. To investigate the impact of pulse modulation on degradation efficiency two key
9 parameters were considered: the duty cycle and period of the pulse modulation envelope. The
10 influence of duty cycle, which is expressed as a percentage of plasma 'on' time to the signal's
11 period was considered. In this investigation, duty cycles of 25 %, 50 % and 75 % were
12 examined. Figure 2(b) shows a 50 % duty cycle case with a period ~20 ms. In all pulse
13 modulated cases, the plasma 'on' power was 5 W. The average power of pulse modulated
14 tests was therefore proportional to the duty cycle and their test time was adjusted accordingly;
15 for example, the 50 % duty cycle case had an average power of 2.5 W and was therefore run
16 for 12 minutes. The rationale for investigating multiple 'on' times comes from the anticipated
17 differences in formation time of reactive species, which evolve on a millisecond timescale [16,
18 17]. Pulse modulated cases with periods of 2 ms, 20 ms and 2 minutes were considered; with
19 the exception of the 25 % duty cycle case with a period of 2 ms, as it was found that plasma
20 could not be generated with an 'on' time of less than 1 ms. Table 1 summarizes the
21 experimental conditions considered.

Condition	Mean Power (W)	Duty Cycle (%)	Period (s)	Test Duration (min)
1	10	100	-	3
2	5	100	-	6
3	2.5	100	-	12
4	3.75	75	0.002, 0.02, 120	9
5	2.5	50	0.002, 0.02, 120	12
6	1.25	25	0.02, 120	24

22 Table 1: Table showing experimental conditions

23 Decolorization was determined by:

$$D = \frac{A_0 - A}{A_0} \times 100\% \quad [\text{Eqn 1}]$$

where D is decolorization, A is the measured absorbance at MO's maximum peak of 664 nm and A_0 is the measured reference absorbance with no decolorization. Since all tests were conducted with the same total energy, volume and dye concentration, efficiency (in g/kW·h) is proportional to decolorization:

$$\text{Efficiency} = D \cdot \frac{C \cdot V}{E} = 0.48D \quad [\text{Eqn 2}]$$

where D is decolorization (expressed as a ratio, $0 \leq D \leq 1$) and C , V and E are the dye concentration, sample volume and total consumed energy, respectively.

Ozone concentration was determined by UV absorbance at 253.37 nm. In all cases a path length of 3 cm was used and the absorption cross-section for Ozone was assumed to be $114.7 \times 10^{-20} \text{ mol}^{-1} \cdot \text{cm}^2$ at 253.65 nm as proposed by Hearn [18]. Other reactive species present in the gas phase were analyzed in-situ using a JASCO FT/IR 4200 system with the plasma generating electrodes inserted within a 10 cm path length gas cell. To obtain a measurement the discharge was sealed within the cell and energized for 2 minutes prior to making to recording data.

The concentration of nitrite and nitrate in solution was determined by treating pure DI water in the reactor under the same plasma conditions as those used for the dye degradation. A Dionex 120 Ion Chromatograph employing a IonPac AS9-HC Carbonate Eluent Anion-Exchange column was used to determine both nitrate and nitrite concentration. In each case, 25 μL of the treated solution was sampled and peak retention time was used to confirm the identity and the peak height used to calculate concentration.

To determine the relative concentration of ionic compounds generated in solution, the pH and conductivity were measured using a Hanna pH meter and a Hanna conductivity meter, respectively. It is a well-established pattern for the conductivity of a plasma treated water sample to rise with treatment time and for the pH to lower [11, 12, 13]. It has been reported that the semi products of MO include acids and ionic compounds; these semi products are likely partially responsible for the post treatment change in conductivity and pH [4, 13]. To establish the relative concentrations of ionic compounds generated solely by the SBD reactor,

1 12 mL samples of DI water were treated and their pH and conductivity were measured
2 immediately after each test.

3

4 **3. Results and discussion**

5 *3.1 Dye decolorization*

6 The decolorization of organic dye using plasma is a complex process involving the generation
7 of active species by the plasma discharge, the transport of those species to the liquid layer,
8 breakdown of dye molecules into intermediate products and the competition between those
9 products for active species. The tests conducted in this investigation employed no forced
10 stirring; hence, mixing in the reactor was limited to diffusion only. Figure 3 highlights the
11 degradation efficiency of MO under the different plasma generation conditions detailed in table
12 1. Critically, it is observed that reducing the duty cycle whilst maintaining a constant input
13 energy can double the overall degradation efficiency, up to an improvement of 2.11 times with
14 a 25 % duty cycle. These results can be partly explained by considering the densities of gas
15 phase reactive species during the plasma on and off times. During the plasma on time the
16 density of many reactive species in the reactor increase rapidly while in the plasma off time,
17 many of the production pathways of such species are eliminated while the loss pathways
18 remain, resulting in a decay of species. Given the long half-life of some reactive species
19 present in the reactor, such as O₃ and H₂O₂, it is reasonable to assume that the decolorization
20 effect of such species is still present after the plasma is extinguished. As the 25 % duty cycle
21 test involves the sample being held in the treatment reactor four times longer than in the
22 continuous case, it is likely that longer lived plasma species remaining during the plasma off
23 time contribute to the overall degradation effect. Interestingly, samples treated with continuous
24 plasma at 5 W for 6 minutes and left to sit undisturbed in the treatment reactor for a further 18
25 minutes, such that the time in the reactor is equivalent to that of a 25 % duty cycle test, showed
26 no obvious improvement in degradation efficiency. This result indicates that the enhanced
27 efficiency observed when pulse modulation is employed is not solely due to samples being
28 held in the reactor for a longer time.

29 The results for the various pulse-modulated cases show that the period of the pulse modulation
30 envelope does not have a noticeable effect on the degradation efficiency. This is an
31 unexpected result. It was hypothesized that short plasma on-times could potentially offer
32 access to alternative discharge chemistries as it is known that the generation of reactive
33 plasma species can take several ms to reach equilibrium [16]. Under the experimental
34 conditions considered in this investigation it is clear that no benefit is gained by using short

1 plasma-on times, indicating that the discharge chemistry has reached equilibrium << 1 ms,
2 which is beyond the shortest plasma-on time considered.

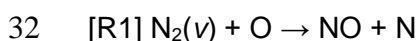
3 An increase in input power, under continuous operation (100 % duty cycle), showed a slight
4 decrease in degradation efficiency. These results can be attributed, in part, to the dynamics of
5 ozone generation, discussed in the following section. Finally, further absorbance
6 measurements conducted 24 hours after plasma treatment indicated that further decolorization
7 occurred by up to 10 %; indicating that long-lived reactive species are dissolved in the sample
8 and play a role in decolorization long after the sample is removed from the reactor.

9

10 *3.2 Reaction kinetics in the plasma, gas and liquid phase.*

11 As this study considered the use of a non-contact surface discharge reactor the primary
12 degradation pathway is likely to be through oxidation by long-lived reactive plasma species,
13 especially ozone [19]. As air is used as the working gas, the production of ozone is affected
14 by plasma power and ozone-quenching gases such as nitrogen oxides [20]. Degradation
15 efficiency is also affected by the residence time of the ozone inside the reactor and the ozone
16 absorption rate of the sample solution. Using a zero-dimensional air plasma model and
17 considering the diffusion of neutral species to the gas phase, Sakiyama *et al.* showed that
18 highly reactive species such as O and OH are rapidly quenched within ~100 ns. Additionally,
19 O and OH are predominantly produced through dissociation by energetic electrons in the
20 plasma phase, there are few energetic electrons beyond the visible discharge hence little
21 additional O or OH is produced in the gas phase. In essence, it can be concluded that the
22 highly reactive short lived plasma generated species do not play a direct role in the dye
23 degradation process [17].

24 Figure 4 shows in-situ FTIR measurements obtained with the discharge operating in a sealed
25 gas cell at 5 W and 10 W. From the figure it is clear that the production of gas phase species
26 varies significantly with the dissipated plasma power. At an operating power of 5 W the gas
27 phase chemistry is dominated by Ozone. As the plasma power is increased to 10 W, the
28 discharge chemistry becomes increasingly dominated by Nitrogen based species, including:
29 N₂O, N₂O₄, N₂O₅, HNO₂ and HNO₃. Critically, in atmospheric pressure air plasma, the creation
30 of NO is known to occur through the reaction of vibrationally-excited nitrogen molecules N₂ (ν)
31 and oxygen atoms (reactions R1 – R3) [20], this limits the density of O available to form ozone.





3 As the discharge power is increased from 5 W to 10 W, the vibrational temperature of Nitrogen
 4 increases which clearly initiates the transition to an ozone-poisoning mode; these results are
 5 highly consistent with previous reports on the poisoning effect of NO on O_3 [20, 21].

6 With low plasma power, the concentration of ozone in the gas phase is high and its flux to the
 7 liquid layer is also significant; yet, recent studies focusing on similar discharges in contact with
 8 water have indicated that the concentration of aqueous O_3 is relatively low [22]. This is due in
 9 part to the relatively low Henry's law constant of O_3 coupled with rapid reactions occurring at
 10 the gas-liquid interface. Table 2 shows the main reactions for O_3 destruction at the gas-liquid
 11 interface. Many of the products formed in these interface reactions are precursors for the
 12 production of Reactive Oxygen Species (ROS) and Reactive Nitrogen Species (RNS) in the
 13 bulk liquid that play a significant role in the decolorization process.

Reaction	Rate coefficient [$M^{-1}s^{-1}$]	ref
$O_3 + OH^- \Rightarrow O_2 + HO_2^-$	40	[23]
$O_3 + OH^- \Rightarrow O_2^- + HO_2$	70	[24]
$O_3 + O^- \Rightarrow O_2^- + O_2$	5.0×10^9	[25]
$O_3 + O_2^- \Rightarrow O_3^- + O_2$	1.6×10^9	[23]
$O_3 + HO_2^- \Rightarrow O_2^- + O_2 + OH$	5.5×10^6	[23]
$O_3 + OH \Rightarrow HO_2 + O_2$	3×10^9	[23]
$O_3 + HO_2 \Rightarrow O_2 + HO_3$	5.0×10^8	[25]
$O_3 + HO_2 \Rightarrow OH + 2O_2$	1.0×10^4	[26]
$O_3 + H_2O_2 \Rightarrow OH + HO_2 + O_2$	6.5×10^{-3}	[26]
$O_3 + H \Rightarrow HO_3$	3.8×10^{10}	[25]
$O_3 + NO_2^- \Rightarrow O_2 + NO_3^-$	$5 \times 10^5 \exp(-6950/T_w)$	[26]

14 Table 2: Table showing experimental conditions

15 To assess the impact of plasma generation conditions on the production of O_3 the time
 16 evolution of O_3 in the reactor was measured, as shown in Figure 5. In the 100 %, 75 % and
 17 50 % duty cycle tests, the concentration of ozone in the reactor peaked after a given time
 18 (dependent on plasma conditions) followed by a decay. In the 25 % duty cycle tests the curve
 19 plateaus with no perceptible downward slope. This downwards trend is attributed to a reduction
 20 in the ozone production rate at the elevated temperatures associated with higher power
 21 operation, increased thermal decomposition of ozone and enhanced quenching by nitrogen
 22 oxides.

1 The peak ozone concentration in the 25 % duty cycle test is approximately 50 % lower than
2 that observed in the 5 W, 100 % duty cycle test; however, this lower level is maintained
3 indefinitely for the duration of the 24 minute test. It is clear to see that as duty cycle increases,
4 the peak level of ozone inside the reaction chamber increases but is accompanied with an
5 increasingly rapid decay. Given that the 25 % duty cycle test establishes a condition where the
6 sample solution is exposed to a high level of ozone for the entire duration of the test, it is clear
7 to see why this is the most effective test condition. A longer exposure to ozone and a
8 decreased concentration of nitrogen oxides that would otherwise compete with dye particles
9 for ROS can partly explain the two-fold increase in degradation efficiency. In the 7.5 W and 10
10 W continuous cases, ozone generation was severely restricted compared to the 5 W case.
11 These observations are consistent with those of the dye degradation efficiency shown in figure
12 3.

13 While ozone is clearly important in the gas phase, its relatively low concentration in solution
14 indicates that it is not the primary agent responsible for the decolorization process. In the bulk
15 liquid, hydrogen peroxide concentration is relatively high in comparison to other ROS species
16 thus suggesting it may play a significant role. This hypothesis is in line with the findings of other
17 plasma-based AOP studies [27, 28], and, given the relatively long lifetime of H_2O_2 in solution,
18 it can partly explain the post-treatment decolorization observed. Consequently, it can be
19 concluded that in an SBD reactor, ozone is a critical intermediary specie and changes made
20 to the plasma-generating waveform that enhance ozone production will translate to enhanced
21 degradation efficiency. This finding is in line with both the measured ozone density under pulse
22 modulated plasma generation and the observed two-fold increase in dye degradation.

23 *3.3 Concentration of nitrogen oxides*

24 As discussed in the previous section, NO production is undesirable due to its poisoning effect
25 on O_3 ; however, in the context of an industrially-viable plasma-based AOP NO production has
26 a second important repercussion. For real-life scenarios where treated water is released back
27 in to the environment, strict rules are in place on the allowable level of dissolved nitrates and
28 nitrites [29, 30]. From figure 4, it is clear that NO_x species generated by the plasma are present
29 in the gas phase; their concentration increases dramatically with increasing discharge power.
30 In the liquid phase, species such as HNO_2 dissociate to form NO_2^- which reacts with O_3 to form
31 NO_3^- .

32 To confirm the hypothesis that the generation of large concentrations of NO_x species in the
33 gas phase leads to nitrate and nitrite formation in solution, the nitrate and nitrite concentration
34 in plasma-treated DI water samples was measured. Figure 6 shows the concentration after

1 exposure to both pulse-modulated and continuously-generated plasma. As the plasma power
2 was increased, the concentration of both nitrate and nitrates in solution increases; this is in-
3 line with the FTIR results highlighted in figure 4. Given that the EU Nitrates Directive
4 (91/676/EEC) indicates that nitrate concentrations of 50 ppm and above are a cause for
5 concern in both surface and groundwater, it is clear that plasma based AOP's operating in air
6 have the potential to produce problematic levels of contamination; pulse modulation of the
7 discharge minimizes this hence offers a means to greatly improve the final water quality.

8 *3.4 pH and conductivity*

9 In addition to contaminating the treated water with nitrates and nitrites, plasma reactors
10 typically generate other undesirable compounds such as acids. These ionic compounds
11 increase conductivity and decrease the pH of the treated solution, as is depicted in figure 7.
12 The decrease in pH can be partly explained by the formation of nitrogen oxides, as outlined in
13 the previous section, and their subsequent dissolution into water leading to nitrite NO_2^- and
14 nitrate ions NO_3^- . These, in turn, form nitric acid HNO_3 and peroxy nitrous acid ONOOH [31].

15 Although the SBD used in this study follows the same pattern as other plasma systems, the
16 lowest power case (25 % duty cycle) registered the smallest change in conductivity and pH
17 despite being the most effective at degrading MO. This indicates that pulse modulation of the
18 discharge can lead to enhanced discharge chemistry: in this case reducing the production of
19 nitrogen oxides while maintaining ozone production.

20 **5. Summary**

21 Decolorization of the organic dye methyl orange was examined using a surface barrier
22 discharge reactor at various excitation duty cycles, periods and power settings. It was found
23 that degradation efficiency for pulse modulated cases, *i.e.* those with duty cycles of less than
24 100 %, was significantly higher than cases in which continuous sinusoidal excitation was
25 employed. It was demonstrated that dye degradation efficiency can be more than doubled
26 when using a pulse modulation duty cycle of 25 % compared to continuously generated plasma.
27 The period of the pulse modulated signal was determined to not have a significant impact on
28 dye decolorization efficiency.

29 Measurements of ozone evolution in the reactor showed that the concentration of ozone
30 reaches a peak shortly after plasma ignition, followed by a period of decay; with the rate of
31 decay being linked to an increase in plasma temperature and elevated NO production.
32 Although the peak ozone concentration was found to be lower in the pulse modulated cases,

1 the decay rate was also lower, with the 25 % duty case showing only a very slight reduction
2 over the duration of the test. In conclusion, improvements in the degradation efficiency when
3 using pulse-modulation excitation can be attributed to: (1) the sample having a longer
4 residence time in the reactor thus allowing for greater absorption of long-lived reactive species,
5 (2) the reduction of gas heating leading to an increase in O₃ production coupled with reduced
6 thermal decomposition and (3) a reduced production of NO and subsequent poisoning of the
7 ozone formation process. Pulse modulation period did not have a significant effect on the
8 degradation efficiency, suggesting that the plasma species in the reactor have already reached
9 equilibrium within 2 ms.

10 Pulse-modulated tests produced a reduced concentration of nitrites, nitrates and other ionic
11 compounds when compared with continuous-wave tests. In the best case, nitrate
12 concentration in the sample was reduced by a factor of 22 when compared to continuously-
13 generated plasma. From the results of this study it is clear that manipulation of the electrical
14 excitation, specifically via pulse modulation, is a highly effective means to enhance the
15 efficiency of plasma mediated breakdown of organic contamination in water. Additionally, this
16 improvement is achieved whilst simultaneously improving the quality of water such that it is
17 suitable for discharge without further processing. Based on these conclusions it is clear that
18 pulse modulation offers several benefits; however, for an industrially viable water-treatment
19 system based upon pulse modulated SBD technology a trade-off would need to be reached
20 between energy efficiency and treatment time.

21

22 **Acknowledgments**

23 The authors would like to thank the UK EPSRC (Grant No. EP/J005894/1) and the NSF Council
24 of China (Grant No. 51307134) for their funding support.

25

26 **References**

27 [1] P.C. Vandevivere, R.B. Bianchi, and W. Verstraete. Treatment and reuse of wastewater
28 from the textile wet-processing industry: Review of emerging technologies. J. Chem.
29 Technol. Biotechnol. 72 (1998) 289-302.

- 1 [2] L.R. Grabowski, E.M. van Veldhuizen, A.J.M. Pemen, and W.R. Rutgers. Corona above
2 water reactor for systematic study of aqueous phenol degradation. *Plasma Chem. Plasma*
3 *Process.* 26 (2006) 3-17.
- 4 [3] L.R. Grabowski, E.M. van Veldhuizen, and W.R. Rutgers. Removal of phenol from water:
5 A comparison of energization methods. *J. Adv. Oxid. Technol.* 8 (2005) 142-149.
- 6 [4] F. Huang, L. Chen, H. Wang, and Z. Yan. Analysis of the degradation mechanism of
7 methylene blue by atmospheric pressure dielectric barrier plasma. *Chem. Eng. J.* 162 (2010)
8 250-256.
- 9 [5] K.T. Byun and H.Y. Kwak. Degradation of methylene blue under multi-bubble
10 sonoluminescence condition. *J. Photochem. Photobiol.* 175 (2005) 45-50.
- 11 [6] D. Gerrity, B.D. Stanford, R.A. Trenholm, and S.A. Snyder. An evaluation of a pilot-scale
12 nonthermal plasma advanced oxidation process for trace organic compound degradation.
13 *Water Res.* 44 (2010) 493-504.
- 14 [7] B. R. Locke, M. Sato, P. Sunka, M. R. Hoffmann, J.-S. Chang. Electrohydraulic discharge
15 and nonthermal plasma for water treatment. *Ind. Eng. Chem. Res.* 45 (2006) 882–905.
- 16 [8] M. Doble and A. Kumar. *Green Chemistry and Engineering*. Elsevier, NY (2007) ISBN:
17 978-0-12-372532-5.
- 18 [9] G. Crini. Non-conventional low-cost adsorbents for dye removal: A review. *Bioresour.*
19 *Technol.* 97 (2006) 1061–1085.
- 20 [10] M.A. Malik. Water purification by plasmas: Which reactors are most energy efficient?
21 *Plasma Chem. Plasma Process.* 30 (2009) 21-31.
- 22 [11] N. Sano, T. Kawashima, J. Fujikawa, T. Fujimoto, T. Kitai, and T. Kanki. Decomposition
23 of organic compounds in water by direct contact of gas corona discharge: Influence of
24 discharge conditions. *Ind. Eng. Chem. Res.* 41 (2002) 5906–5911.
- 25 [12] M. Simek, S. Pekarek, and V. Prukner. Influence of power modulation on ozone
26 production using an ac surface dielectric barrier discharge in oxygen. *Plasma Chem. Plasma*
27 *Process.* 30 (2010) 607-617.
- 28 [13] M. Simek, S. Pekarek, and V. Prukner. Ozone production using a power modulated
29 surface dielectric barrier discharge in dry synthetic air. *Plasma Chem. Plasma Process.* 32
30 (2012) 743-754.
- 31 [14] J.L. Walsh, J.J. Shi, and M.G. Kong. Contrasting characteristics of pulsed and sinusoidal
32 cold atmospheric plasma jets. *Appl. Phys. Lett.*, 88 (2006) 171501.
- 33 [15] F. Massines, N. Gherardi, N. Naude, and P. Segur. Recent advances in the
34 understanding of homogeneous dielectric barrier discharges. *Eur. Phys. J. Appl. Phys.* 47
35 (2008) 22805.
- 36 [16] J.H. Lozano-Parada and W.B. Zimmerman. The role of kinetics in the design of plasma
37 microreactors. *Chem. Eng. Sci.*, 65 (2010) 4925-4930.

- 1 [17] Y. Sakiyama, D.B. Graves, H.W. Chang, T. Shimizu, and G.E. Morfill. Plasma chemistry
2 model of surface microdischarge in humid air and dynamics of reactive neutral species. J.
3 Phys. D: Appl. Phys. 45 (2012) 425201.
- 4 [18] A.G. Hearn. The adsorption of ozone in the ultra-violet and visible regions of the
5 spectrum. Proc. Phys. Soc., 78 (1961) 932-940.
- 6 [19] J. Sakalys and R. Girgždiene. Estimation of the ground-level ozone lifetime under rural
7 conditions. Lith. J. Phys. 50 (2010) 247-254.
- 8 [20] T. Shimizu, Y. Sakiyama, D.B. Graves, J.L. Zimmerman, and G.E. Morfill. The dynamics
9 of ozone generation and mode transition in air surface micro-discharge plasma at
10 atmospheric pressure. New J. Phys. 14 (2012) 103028.
- 11 [21] X.L. Deng, A.Yu. Nikiforov, P. Vanraes, and Ch. Leys. Direct current plasma jet at
12 atmospheric pressure operating in nitrogen and air. J. Appl. Phys. 113 (2013) 023305.
- 13 [22] N. Takeuchi, Y. Ishii and K. Yasuoka. Modelling chemical reactions in dc plasma inside
14 oxygen bubbles in water. Plasma Sources Sci. Technol., 21 (2012) 015006.
- 15 [23] H. Tomiyasu, H. Fukutomi, and G. Gordon. Kinetics and mechanism of ozone
16 decomposition in basic aqueous solution. Inorg. Chem. 24, (1985) 2962-2966.
- 17 [24] S.N. Pandis. J.H. Seinfeld. Sensitivity Analysis of a Chemical Mechanism for Aqueous-
18 Phase Atmospheric Chemistry. J. Geophys. Res-Atmos, 94 (1989) 1105-1126.
- 19 [25] B. Pastina, J.A. LaVerne, Effect of Molecular Hydrogen on Hydrogen Peroxide in Water
20 Radiolysis. J. Phys. Chem. A. 105 (2001) 9316-9322.
- 21 [26] T Shibata and H Nishiyama, Numerical study of chemical reactions in a surface
22 microdischarge tube with mist flow based on experiment. J. Phys. D: Appl. Phys. 47 (2014)
23 105203
- 24 [27] X. Wang, X. Jin, M. Zhou, Y. Liu, and X. Zhang. Decolorization of acid orange 7 with dc
25 diaphragm glow discharge. Electrochim. Acta. 103 (2013) 237–242.
- 26 [28] M.A. Malik, A. Ghaffar, and S.A. Malik. Water purification by electrical discharges.
27 Plasma Sources Sci. Technol. 10 (2001) 82-91.
- 28 [29] M. Karlsson, B. Karlberg, and R.J.O Olsson. Determination of nitrate in municipal waste
29 water by uv spectroscopy. Analytica Chimica Acta, 312 (1995) 107–113.
- 30 [30] S.M. Lee, K.D. Min, N.C.Woo, Y.J. Kim, and C.H. Ahn. Statistical models for the
31 assessment of nitrate contamination in urban groundwater using GIS. Environ. Geol. 44
32 (2003) 210-221.
- 33 [31] J.L. Brisset, B. Benstaali, D. Moussa, J. Fanmoe, and E. Njoyim-Tamungang. Acidity
34 control of plasma-chemical oxidation: applications to dye removal, urban waste abatement
35 and microbial inactivation. Plasma Sources Sci. Technol. 20 (2011) 034021.
- 36
37

1 **Figure Caption:**

2 Figure 1: Diagram of experimental reactor showing superimposed representation of the
3 glass dielectric barrier with copper electrodes attached to either side.

4

5 Figure 2: Typical discharge current and voltage waveforms of the surface discharge: (a)
6 current and voltage waveforms on microsecond timescale, insert showing 20
7 ns exposure iCCD image, (b) voltage waveform on millisecond timescale
8 showing pulse modulation envelope (50 % duty cycle, 20 ms period).

9

10 Figure 3: Energy efficiency with respect to mean plasma power for various duty cycles
11 and periods. Powers below 5 W relate to pulse modulated cases, where the
12 percentage shown indicates duty cycle used.

13

14 Figure 4: In situ absorbance measurements of the gas phase species at plasma powers
15 of 5 W and 10 W. Insert shows the experimental set up.

16

17 Figure 5: Time evolution of ozone concentration in sample enclosure: (a) continuous
18 cases; (b) 75 % duty cycle cases; (c) 50 % duty cycle cases and (d) 25 % duty
19 cycle cases.

20

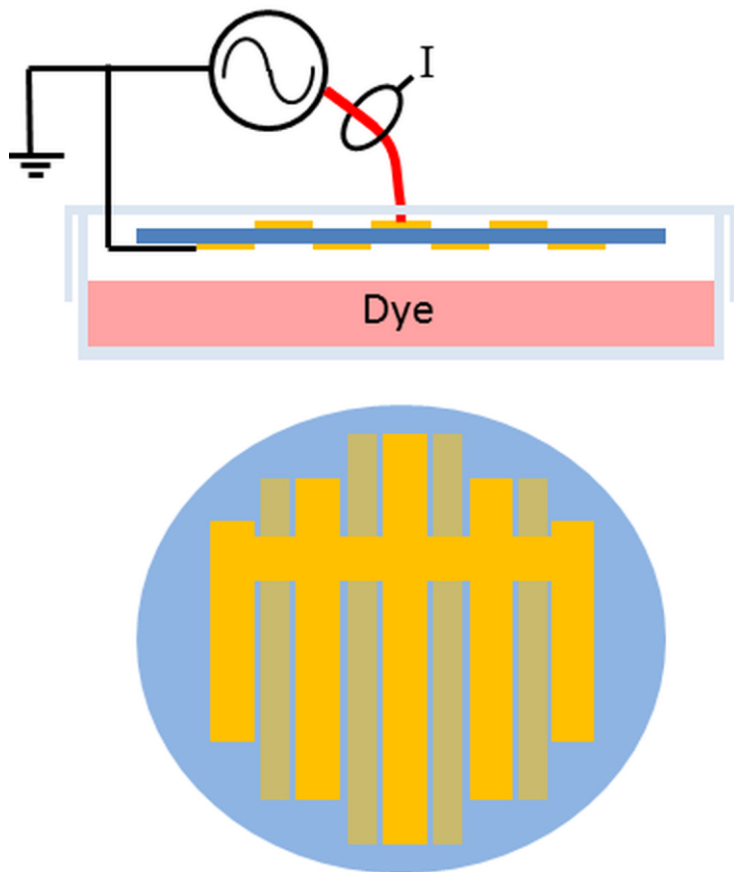
21 Figure 6: Nitrate and nitrite concentration in a distilled water sample post plasma
22 treatment with respect to mean plasma power; percentages indicate duty cycle
23 used.

24

25 Figure 7: Evolution of (a) conductivity and (b) pH of DI water sample, as a function of
26 plasma energy density.

27

28



1
2 Figure 1: Diagram of experimental reactor showing superimposed representation of the
3 glass dielectric barrier with copper electrodes attached to either side.
4

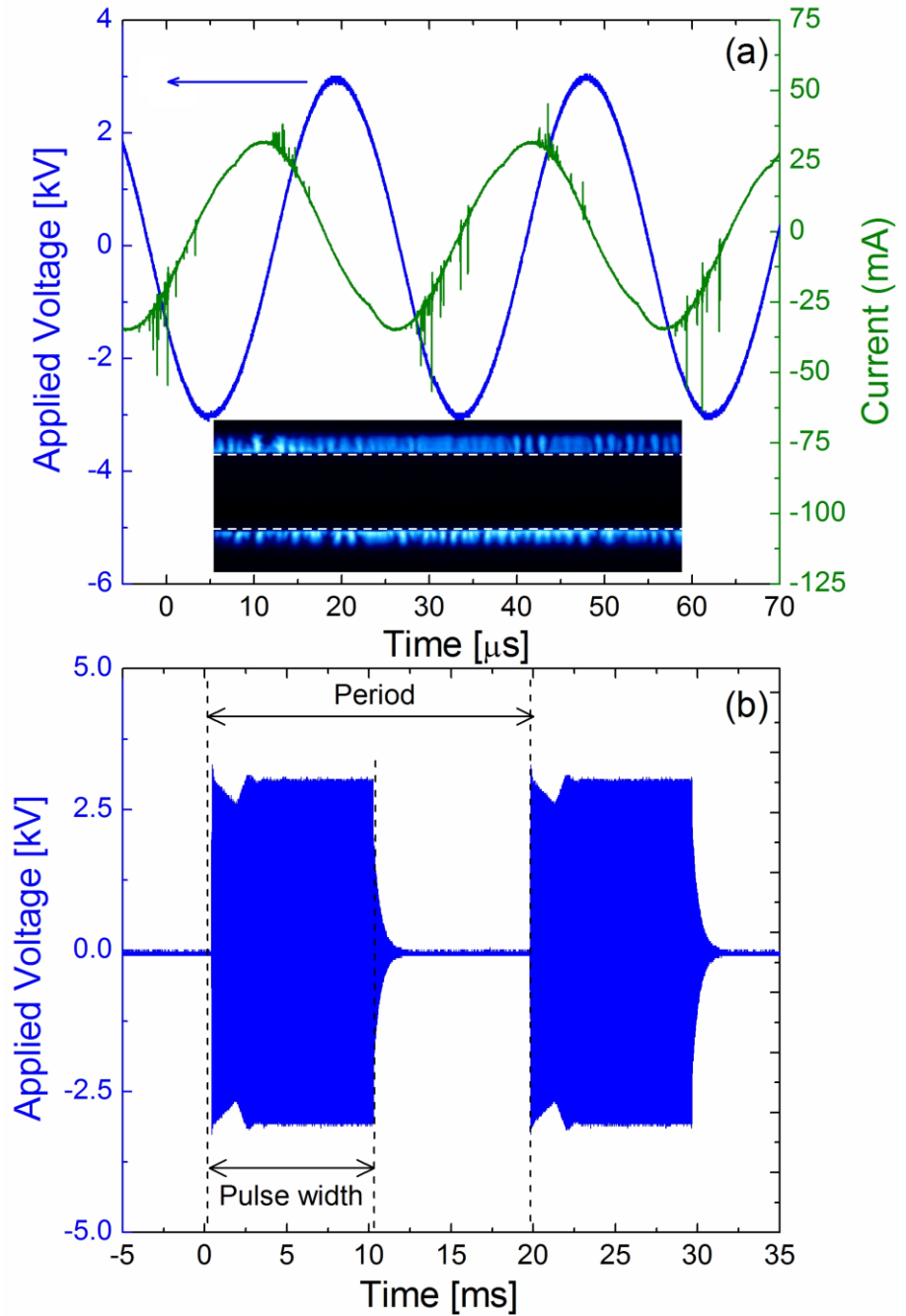
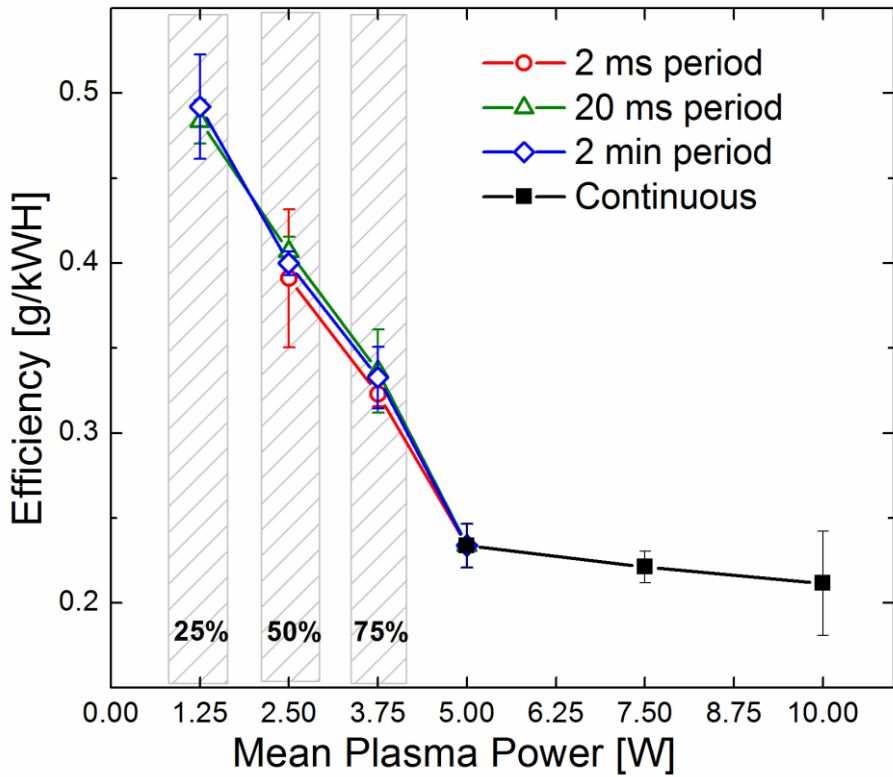


Figure 2: Typical discharge current and voltage waveforms of the surface discharge: (a) current and voltage waveforms on microsecond timescale, insert showing 20 ns exposure iCCD image, (b) voltage waveform on millisecond timescale showing pulse modulation envelope (50 % duty cycle, 20 ms period).

1
2
3
4
5
6
7
8
9
10



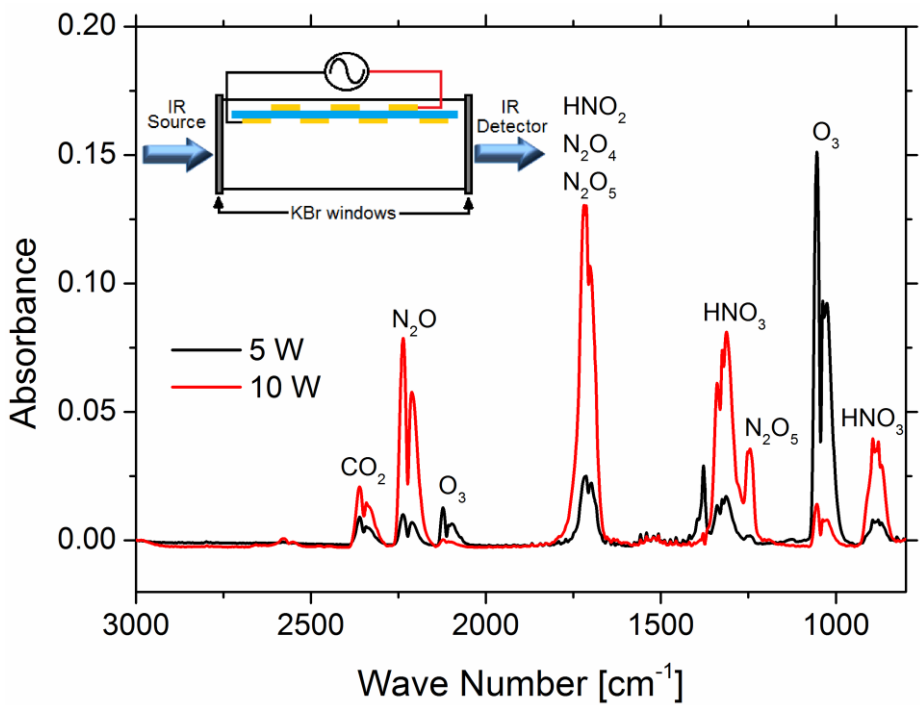
1

2 Figure 3: Energy efficiency with respect to mean plasma power for various duty cycles
3 and periods. Powers below 5 W relate to pulse modulated cases, where the
4 percentage shown indicates duty cycle used.

5

6

7



1
2 Figure 4:
3 *In situ* absorbance measurements of the gas phase species at plasma powers
4 of 5 W and 10 W. Insert shows the experimental set up.

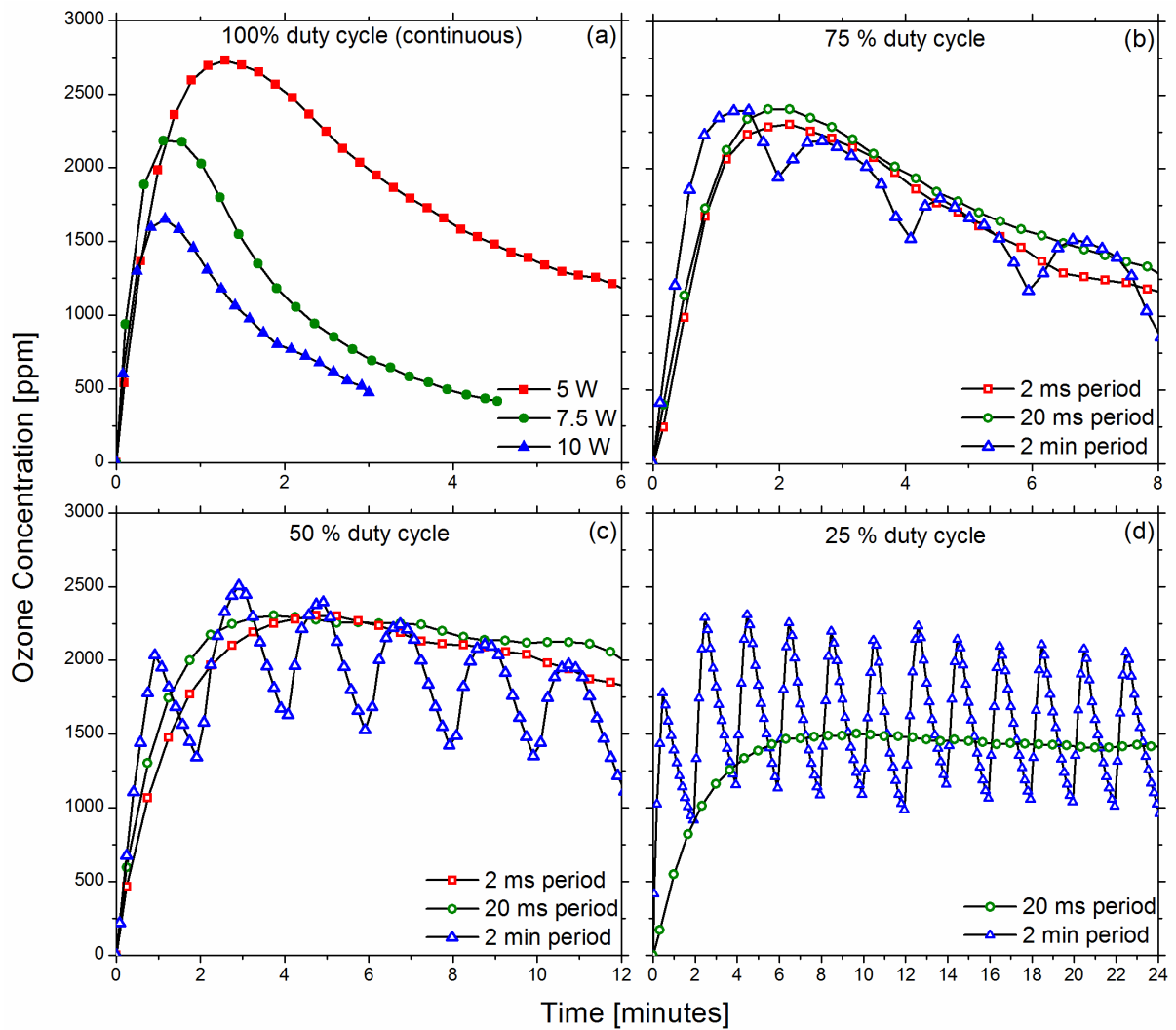


Figure 5: Time evolution of ozone concentration in sample enclosure: (a) continuous cases; (b) 75 % duty cycle cases; (c) 50 % duty cycle cases and (d) 25 % duty cycle cases.

1
2
3
4
5
6
7
8
9
10
11
12
13

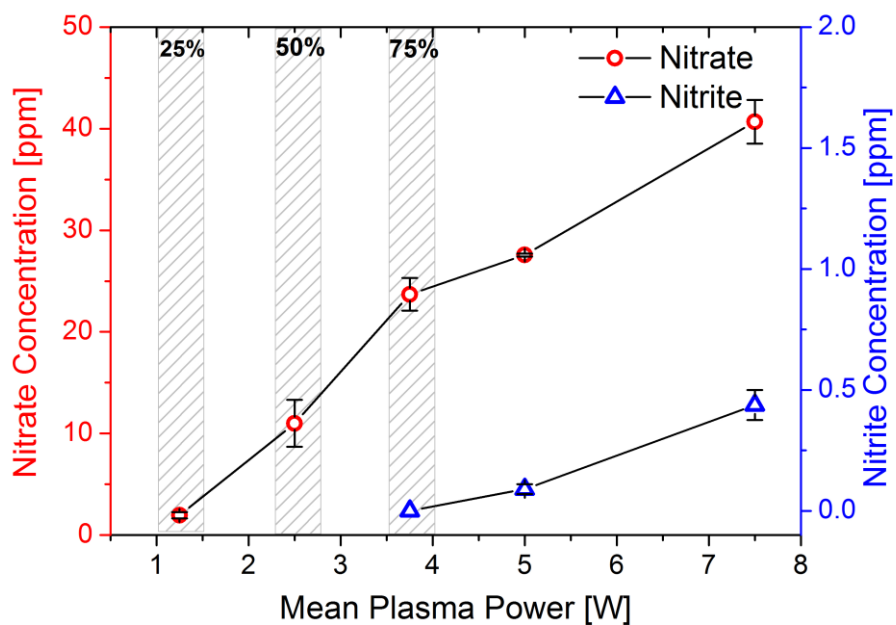
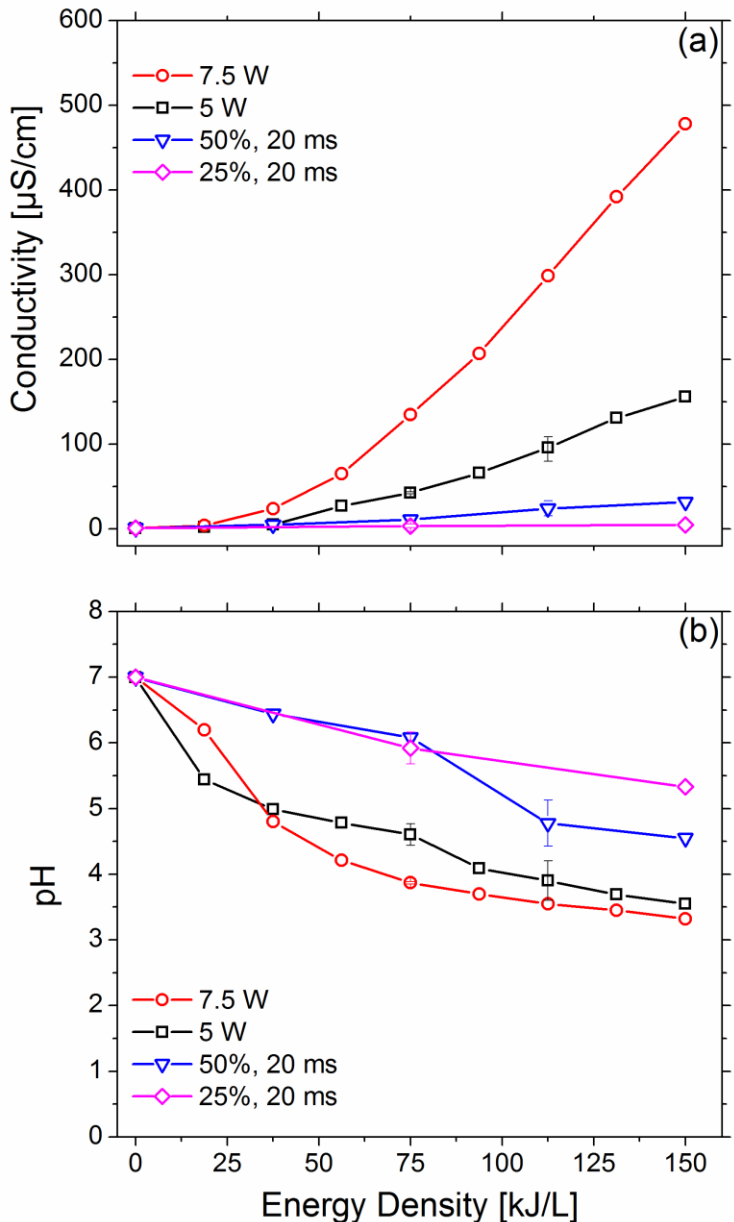


Figure 6: Nitrate and nitrite concentration in a distilled water sample post plasma treatment with respect to mean plasma power; percentages indicate duty cycle used.

1
2
3
4
5
6
7
8
9
10
11
12
13
14
15
16
17
18



1

2 Figure 7: Evolution of (a) conductivity and (b) pH of DI water sample, as a function of
 3 plasma energy density.

4

5

